Electronic Supplementary Information

Enhancing Efficiency and Stability in Inverted Binary Organic Solar Cells through Hydroxylated Perylene Diimide Derivative Cathode Interlayers

Li Tian[a]*#, Lingwei Feng[b]#, Shukui Guo[a], Renjie Wang[a], Kai Zhang[b]*, Cheng-Xing Cui[c]*

[a.]School of Materials Science and Engineering, Henan University of Technology, Zhengzhou 450001, P.R. China,

[b.]Institute of Polymer Optoelectronic Materials and Devices State Key Laboratory of Luminescent Materials and Devices South China University of Technology Guangzhou 510640, P. R. China.

[c.]School of Chemistry and Chemical Engineering, Institute of Computational Chemistry, Henan Institute of Science and Technology, Xinxiang 453003, China

1. Experimental section

Materials: All chemicals without special explanation were brought from Tianjin Kermel Chemical Reagent Co., Ltd. 3,4,9,10-Perylenetetracarboxylic dianhydride, N-(3-Aminopropyl)diethanolamine, 3-diethylaminopropylamine, bromoethane and 2-Bromoethanol were purchased from Energy Chemical and used with no more treatment. 2,9-bis(3-(diethylamino)propyl)anthra[2,1,9-def:6,5,10-d'e'f']diisoquinoline-1,3,8,10(2H,9H)-tetraone (M1) and PDI-Br-0O[1] were synthesized referencing the published literatures.

Synthesis of 2,9-bis(3-(bis(2-hydroxyethyl)amino)propyl)anthra[2,1,9-def:6,5,10-d'e'f']diisoquinoline-1,3,8,10(2H,9H)-tetraone (M2)

In a flask, 3,4,9,10-Perylenetetracarboxylic dianhydride (1.18 g, 3 mmol) was dissolved in 30 mL of N,N-dimethylformamide (DMF), and then N-(3-Aminopropyl)diethanolamine (1.48 g, 9 mmol) was added. The reaction mixture was under nitrogen atmosphere at 130℃ for 3 h. Then, the reaction mixture was poured into methanol and filtered, washed by methanol and dichloromethane, dried under vacuum. Finally, the pure product (M2) was obtained as dark red solid with a yield of 85% (1.72g).

^{1}H NMR (400 MHz, DMSO) δ = 8.90 (s, 4H), 8.58 – 8.46 (m, 4H), 4.16 (s, 4H), 3.26 (s, 13H), 3.01 – 2.89 (m, 4H), 2.08 (s, 4H), 1.19 (t, J=6.9, 18H).

Synthesis of PDI-Br-1O

250 mg of M1 was dissolved in 20 ml toluene and then 2 mL of 2-bromoethanol was added. The mixture was refluxed for 24 h under nitrogen. A large amount of red precipitate was precipitated. The reaction mixture was cooled to room temperature and filtered. The crude product was washed by dichloromethane and methanol. After drying under vacuum, PDI-Br-1O was obtained as a red solid (326 mg, 92%) ESI-MS: m/z calculated for $C_{42}H_{50}Br_2N_4O_6$: 866.2; found: 353.2 [M^{2+}-2Br−]/2

^{1}H NMR (400 MHz, DMSO) δ = 8.90 (s, 4H), 8.58 – 8.46 (m, 4H), 4.16 (s, 4H), 3.26 (s, 13H), 3.01 – 2.89 (m, 4H), 2.08 (s, 4H), 1.19 (t, *J*=6.9, 18H).

^{13}C NMR (101 MHz, DMSO) δ 162.67, 132.90, 131.38, 130.24, 123.81, 121.72, 56.72, 55.43, 51.98, 37.97, 23.27.

Synthesis of PDI-Br-3O

250 mg of M2 was dissolved in 15 ml trifluoroethanol and then 2 mL of 2-bromoethanol was added. The reaction mixture was under nitrogen atmosphere at 60℃ for 72 h. The reaction mixture was cooled to room temperature and then poured into tetrahydrofuran. The solid was collected and re-dissolved in 5 mL of trifluoroethanol again, then precipitated from a mixture of hexane and ethyl acetate. The crude product was washed by dichloromethane. After drying under vacuum, PDI-Br-3O was obtained as a red solid (310 mg, 88%). ESI-MS: m/z calculated for $C_{42}H_{50}Br_2N_4O_{10}$: 930.2; found: 385.2 [$M^{2+}$-2Br−]/2

^{1}H NMR (400 MHz, DMSO) δ = 7.81 (s, 8H), 4.00 (s, 4H), 3.72 (s, 12H), 3.33 (s, 4H), 3.15 (s, 12H), 2.06 (s, 4H).

^{13}C NMR (101 MHz, DMSO) δ 162.67, 132.90, 131.38, 130.24, 123.81, 121.72, 56.72, 55.43, 51.98, 37.97, 23.27.

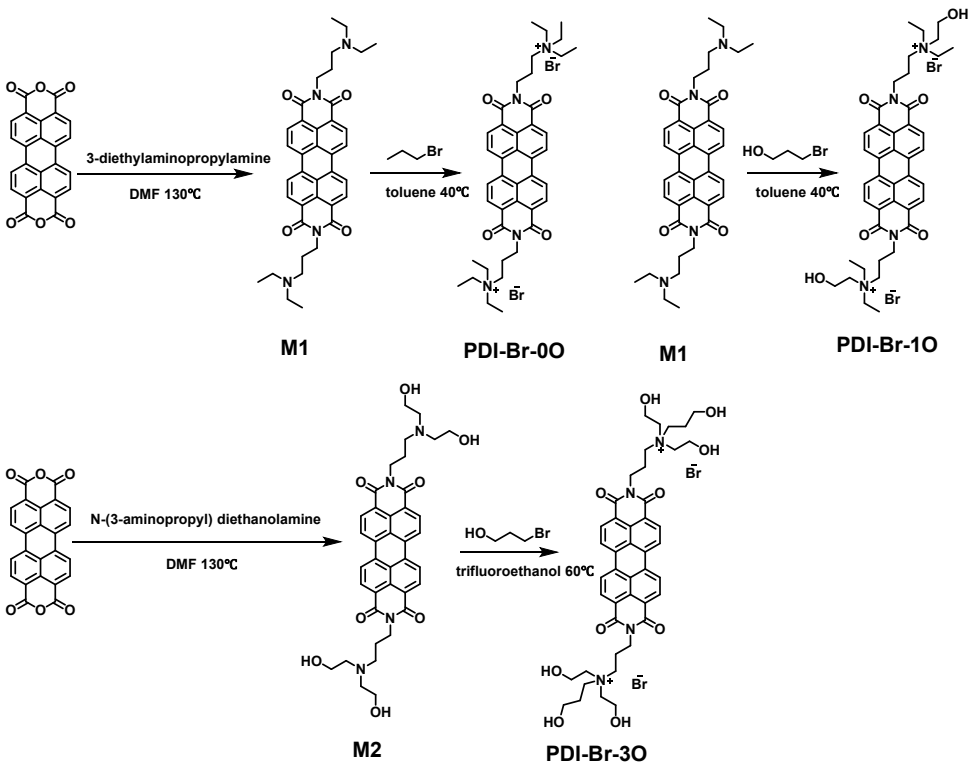

Scheme S1. Synthetic routes of PDI-Br-0O, PDI-Br-1O, and PDI-Br-3O

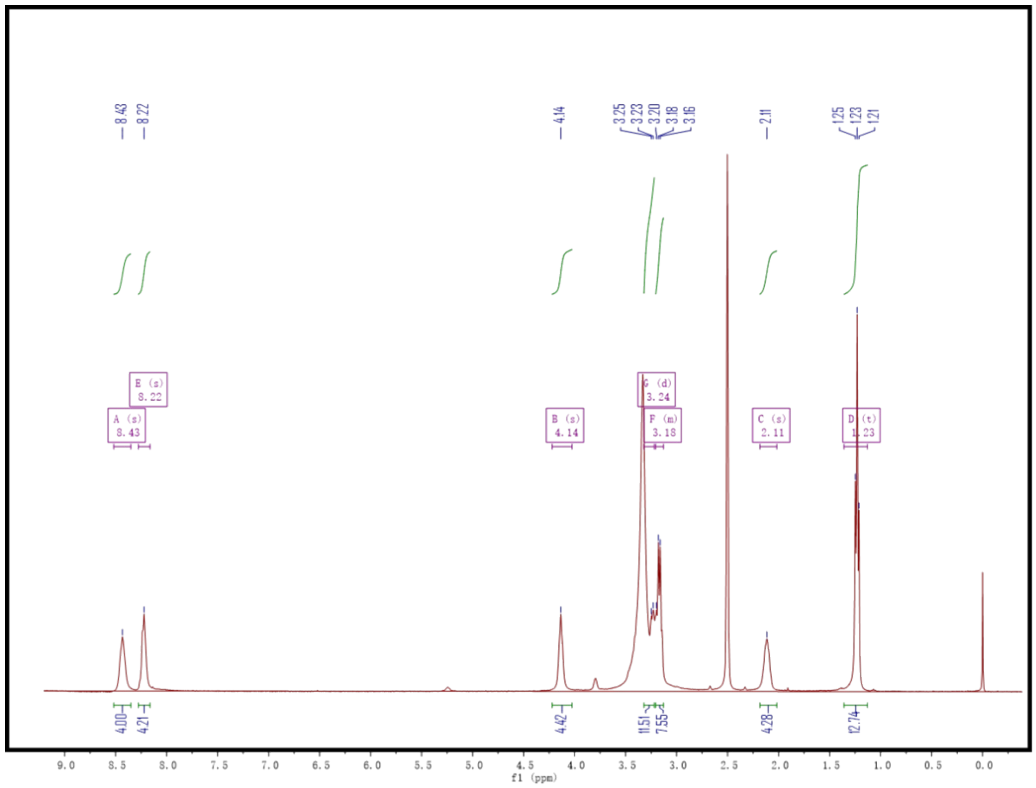

Figure S1 ^{1}H NMR of PDI-Br-1O.

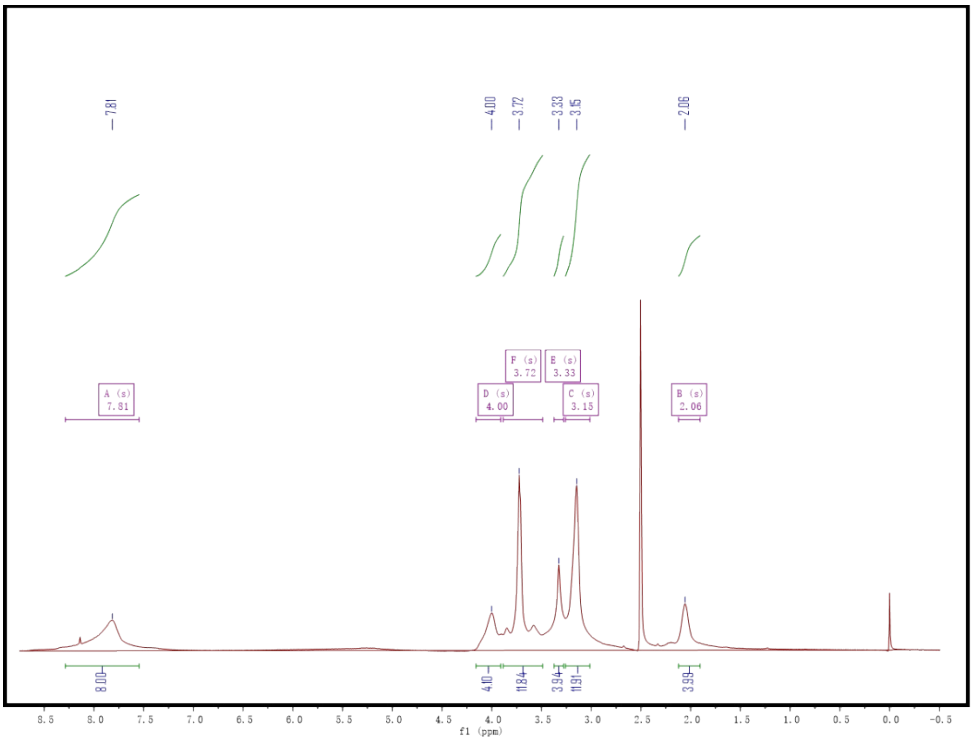

Figure S2 ^{1}H NMR of PDI-Br-3O.

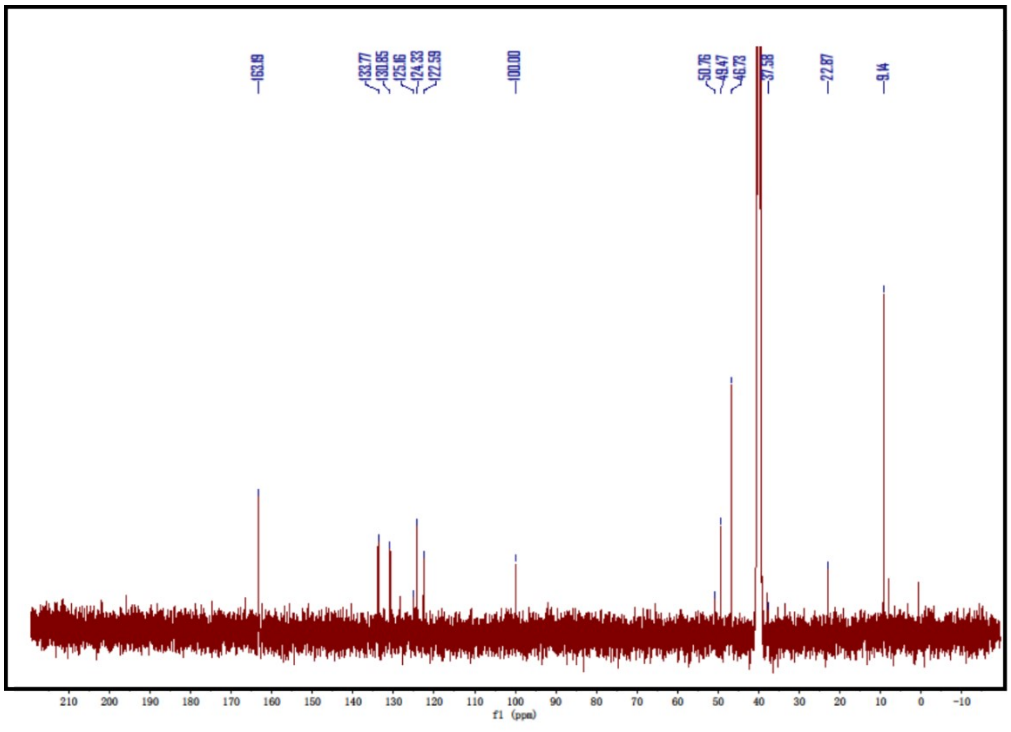

Figure S3 ^{13}C NMR of PDI-Br-1O.

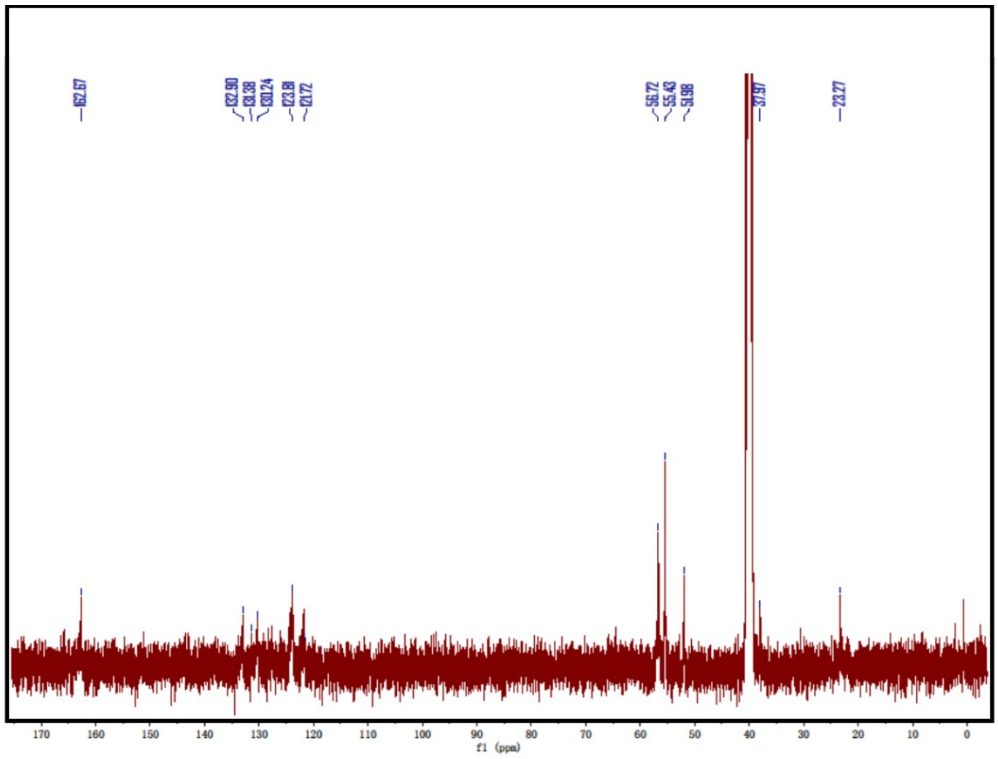

Figure S4 ^{13}C NMR of PDI-Br-3O.

Characterization:

The ^{1}H NMR spectra of monomers were measured by Bruker AVANCE Digital NMR workstation operating at 400 MHz. The UV-vis absorption spectra of these PDI-derivatives were obtained by using HP 8453 spectrophotometer. The CV curves of PDI-derivatives were recorded by CHI660E electrochemical workstation, in a 0.1 M acetonitrile solution of tetrabutylammonium hexafluorophosphate (Bu_4NPF_6) at room temperature. A three-electrode setup was used to record the electrochemical characteristics with ITO electrodes as working electrodes, a saturated calomel electrode (SCE) as the reference electrode, and a platinum wire electrode as the counter electrode. ESR spectroscopies of these polymers were recorded by a JEOL JES-FA200 ESR spectrometer (300 K, 9.063 GHz, Xband) at room temperature. The work functions of Ag electrodes with/without these CILs were measured using the scanning Kelvin probe measurement (SKP 5050, KP Technology) and ultraviolet photoelectron spectroscopy (UPS). The UPS measurements were

performed on the Thermo ESCALAB 250XI. The valance band (VB) spectra were measured with a monochromatic He I light source (21.2 eV) and a VG Scienta R4000 analyzer.

Fabrication and Characterization of OSC devices:

The inverted OSC devices with an architecture of ITO/ETLs/D18:EH-HD-4F/MoO_3/Ag were fabricated. ITO substrates were cleaned with detergent, water and isopropanol for 2 rounds, under ultrasonic bath. After drying, the pre-cleaned ITO-coated glass substrates were UV/ozone-treated for 5 min. For ZnO reference devices, the zinc acetate precursor solution was spin-coated onto the ITO substrates at 3000 rpm for 30s, followed by annealing at 200℃ for 30 min. For PDI-derivatives devices, PDI-derivatives were dissolved in trifluoroethanol with varied concentration, then the solution was spin-coated at 2000 rpm for 30s onto the ITO substrate directly without post-treatment, yield varied thickness. Then, all CIL coated substrates were transferred to the nitrogen-filled glovebox. The active layer was spin-coated at 3000rpm from solutions of D18:EH-HD-4F (weight ratio of 1:1.4) in chloroform with a total concentration of 9.6 mg mL^{-1}. The thickness of active layer was 100 nm. The devices were completed after deposition of 10 nm MoO_3 and 100 nm Ag under vacuum at 9×10^{-7} Torr. The device area was 0.04 cm^2. The $J-V$ characteristics for OSCs were measured under AM 1.5G illumination (100 mW/cm^2) using a solar simulator (Oriel model 91192). The external quantum efficiency (EQE) was measured with a monochromator (Newport, Cornerstone 130) linked to a xenon lamp and a lock-in amplifier (Stanford Research Systems, SR 830) coupled to a light chopper.

Fabrication of electron-only devices

The electron mobility was measured by the space charge limited current (SCLC) method. Electron-only devices with an architecture of ITO/CIL/Ag or ITO/ZnO/CIL (5 nm)/ EH-HD-4F/Ag were

prepared. The *J-V* characteristics for electron-only devices were recorded using AM 1.5G illumination with an intensity of 100mWcm^{-2}.

Stability test.

Storage stability: Devices were stored in glovebox under nitrogen atmosphere with darkness.

Photostability: Devices were encapsulated and tested in the atmospheric environment at room temperature. An array of white LEDs was utilized as the light source and the intensity of light was sketchily calibrated to the same level of device performance under AM 1.5G.

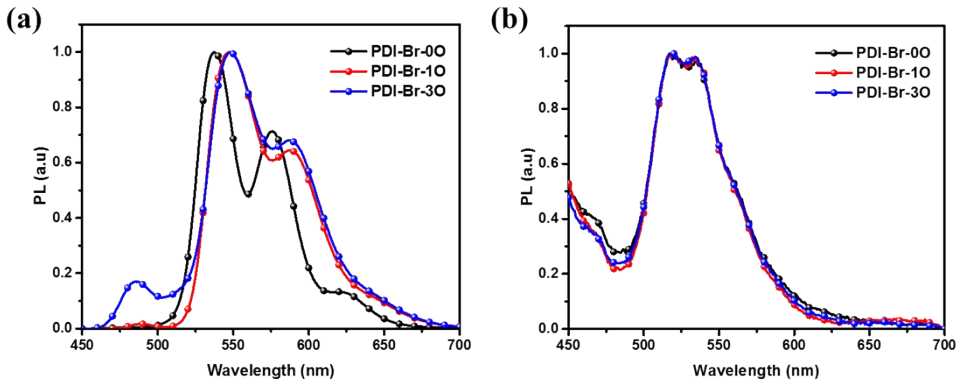

Figure S5 PL spectra of PDI-Br-0O, PDI-Br-1O and PDI-Br-3O (c) in trifluoroethanol and (d) in thin-film state;

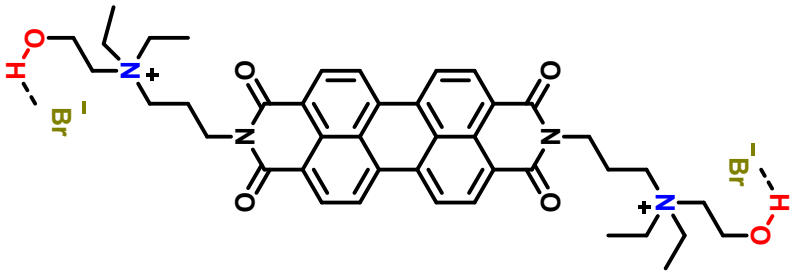

Figure S6 The diagram of hydrogen-like bonds between Br^- and hydroxyl.

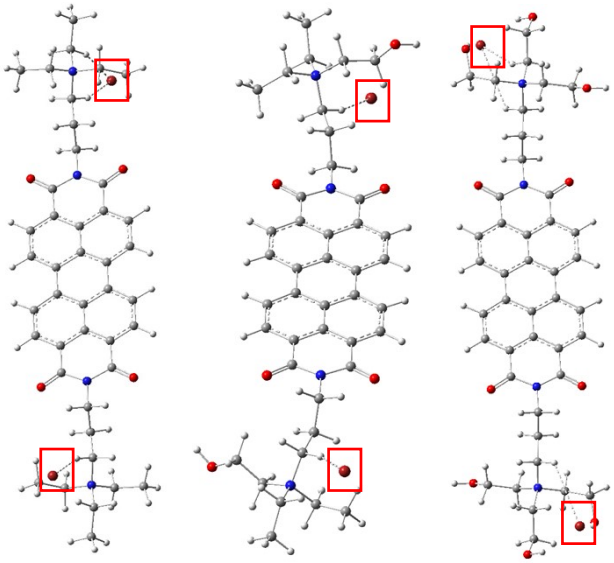

Figure S7. The optimized geometries of PDI-derivatives.

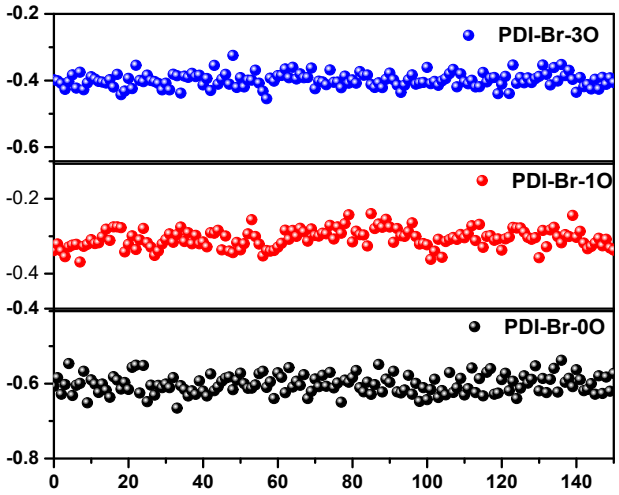

Figure S8 Kelvin probe microscopy (KPM) of ITO/PDI-Br-0O, ITO/PDI-Br-1O, and ITO/PDI-Br-0O versus ITO.

Table S1. Electron mobilities of PDI-derivatives and CIL/EH-HD-4F

CIL	PDI-Br-0O	PDI-Br-1O	PDI-Br-3O	ZnO
Electron mobilities ($cm^2\ V^{-1}\ s^{-1}$)	5.81×10^{-7}	2.28×10^{-6}	2.89×10^{-6}	--
Electron mobilities with EH-HD-4F ($cm^2\ V^{-1}\ s^{-1}$)	--	1.254×10^{-3}	2.737×10^{-3}	1.511×10^{-6}

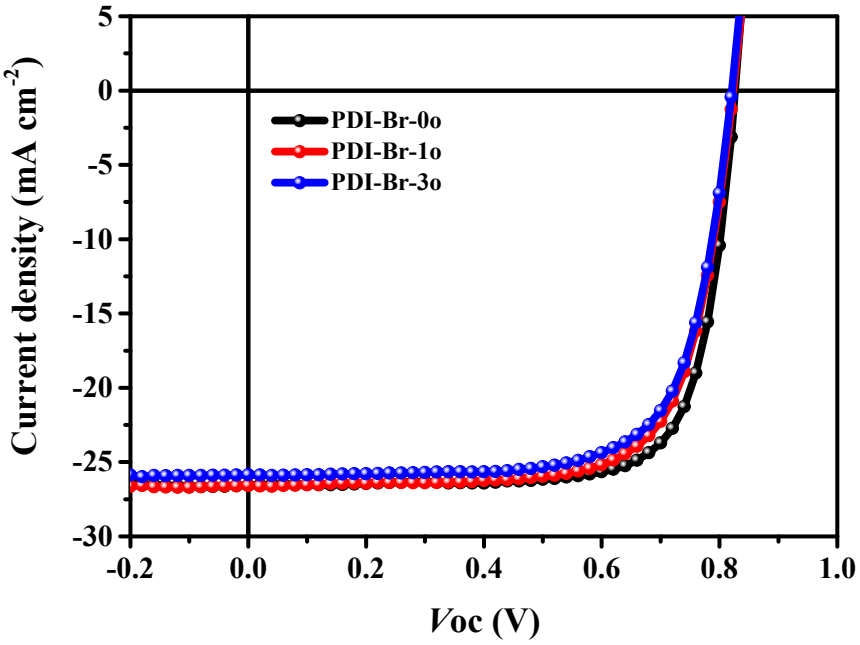

Figure S9. *J–V* curves of conventional OSC devices with PDI-derivatives.

Table S2. Device parameters of conventional OSC devices with PDI-derivatives

	Voc	Jsc	FF	PCE
PDI-0O	0.827±0.001	26.55±0.02	75.25±0.54	16.60(16.53±0.11)
PDI-1O	0.822±0.001	26.51±0.26	72.53±0.36	15.91(15.81±0.10)
PDI-3O	0.820±0.002	25.68±0.25	72.21±0.32	15.28(15.21±0.11)

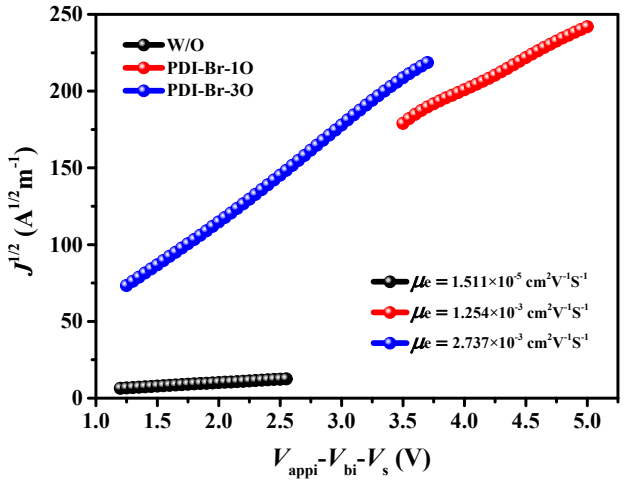

Figure S10. The J–V curves of electron-only devices with ITO/ZnO/ PDI-derivatives (5 nm) / EH-HD-4F/ Ag (100 nm) structures.

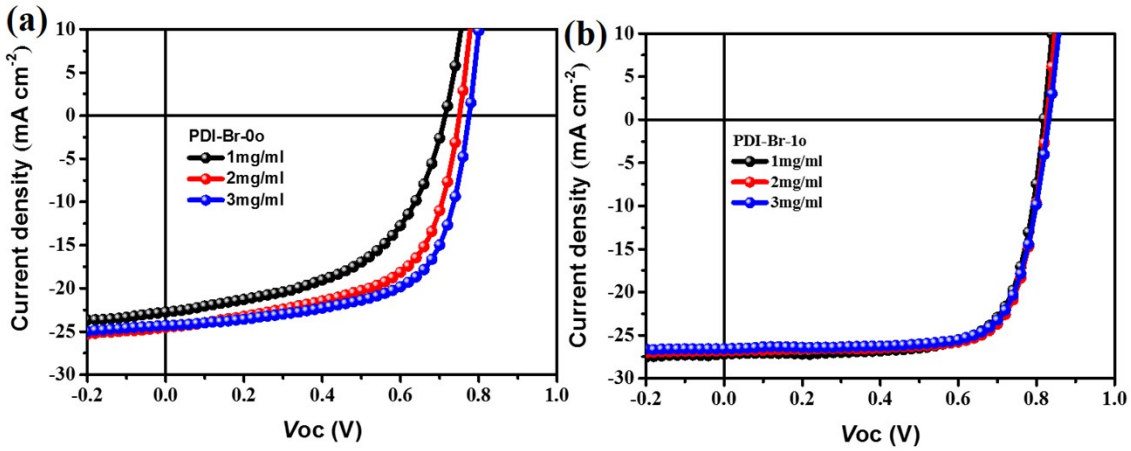

Figure S11. J–V curves of OSC devices with different thicknesses of PDI-Br-0O and PDI-Br-1O.

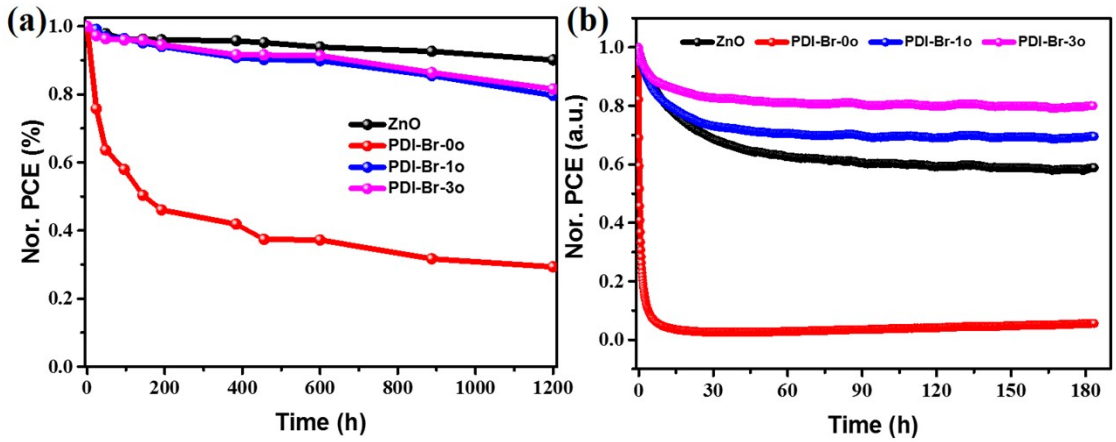

Figure S12. (a) Storage stability test of devices with ZnO, PDI-Br-0O, PDI-Br-1O and PDI-Br-3O -based cells under darkness. (b) Operation stability test of devices with PDI-Br-0O, PDI-Br-1O and PDI-Br-3O under continuous illumination.

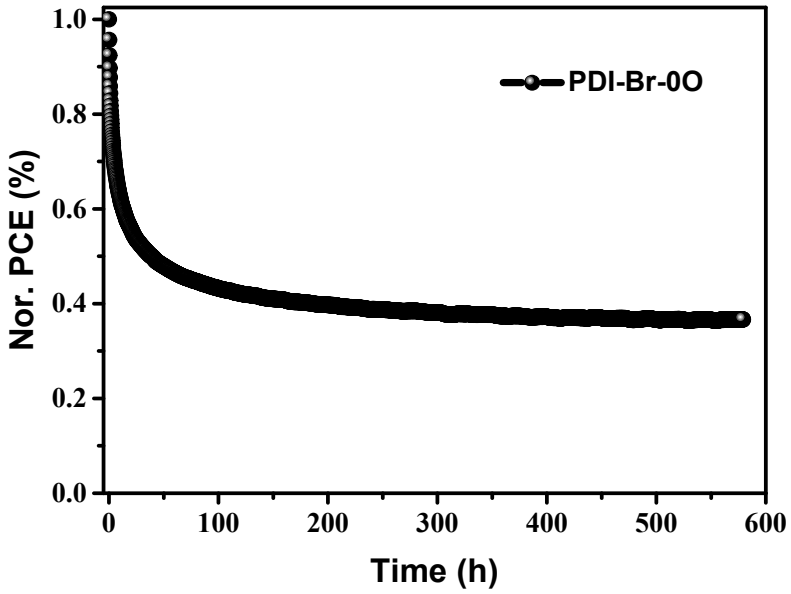

Figure S13. Operation stability test of conventional devices with PDI-Br-0O under continuous illumination.

Reference:

1. B. Wang, C. Yu, Angew. Chem., 2010, 49, 1485-1488.